Phase-Resolved Measurements of Ion Velocity in a Radio-Frequency Sheath

Brett Jacobs,[1,][*] Walter Gekelman,[1] Pat Pribyl,[1] and Michael Barnes[2]

[1]*Department of Physics and Astronomy, University of California—Los Angeles, Los Angeles, California 90024, USA*
[2]*MS Barnes Engineering, San Ramon, California 94583, USA*

The time-dependent argon-ion velocity distribution function above and within the plasma sheath of an rf-biased substrate has been measured using laser-induced fluorescence in a commercial plasma processing tool. Discharge parameters were such that the 2.2 MHz rf-bias period was on the order of the ion transit time through the sheath ($\tau_{\mathrm{ion}}/\tau_{\mathrm{rf}} = 0.3$). This work embodies the first time-resolved measurement of ion velocity distribution functions within an rf-biased sheath over a large area (30 cm diameter) silicon wafer substrate.

Low pressure (0.5 to 10 mTorr) plasmas (densities 10^{10} to 10^{12} cm^{-3}) are used extensively to process materials and are vital to the fabrication of semiconductor integrated circuits [1]. The formation of small features across a large area substrate requires precise control and uniformity of the plasma parameters. Historically, the development of these processes has been empirically "recipe driven" where trial and error in conjunction with previous experience plays a major role in development. The improvement of plasma diagnostics has made it possible to directly measure parameters critically related to plasma processing [2]. Advances in modeling have also provided symbiotic avenues for enhanced understanding of industrial plasmas [3]. We report time-resolved laser-induced fluorescence (LIF) measurements of the argon-ion velocity distribution function (IVDF) in the presheath and sheath region when an rf-bias voltage is applied to a substrate by a capacitive applicator in a commercial plasma processing device. The rf bias creates an expanded sheath region which accelerates ions to the substrate. These measurements will play an important role in the design of future generation plasma devices and processing regimes, and provide benchmarks for theoretical models.

The use of LIF as a plasma ion diagnostic was first popularized by Stern and Johnson [4]. The first experiments used low power cw lasers and signal averaging to study plasma rotation [5] and low-frequency waves [6]. Since then, many basic plasma physics experiments have employed this technique and a lengthy review paper would be required to cite them. The LIF technique was adapted for measurements in plasma processing reactors [2]; measurements of the ion distribution function were made in the presheath [7,8] (region separating the bulk plasma and the narrow sheath above the substrate) and sheath [9] in the absence of substrate bias voltage. Time-averaged, spatially resolved measurements were obtained in the biased sheath above an electrode in a capacitively coupled nitrogen discharge; the plasma density was also evaluated [10].

The ion dynamics within rf sheaths critically depends upon the ratio of the ion transit time through the sheath to the rf period ($\tau_{\mathrm{ion}}/\tau_{\mathrm{rf}}$) [11]. In the high-frequency regime ($\tau_{\mathrm{ion}}/\tau_{\mathrm{rf}} \gg 1$), sheath models show that the ions respond to the time-averaged sheath fields and the IVDF is narrow and roughly independent of time during an rf cycle. Conversely, in the low-frequency regime ($\tau_{\mathrm{ion}}/\tau_{\mathrm{rf}} \ll 1$), ions quickly respond to the full time-dependent sheath fields which give a collection of IVDFs which, when time averaged, are broad and bimodal. The intermediate frequency regime is the most complicated, where the inertia of the ions cause them to partially respond to the oscillating sheath fields. In this experiment, the rf-bias power and frequency were chosen such that the ratio of the calculated ion transit time through the sheath to the rf period $\tau_{\mathrm{ion}}/\tau_{\mathrm{rf}} = 0.3$.

The LIF measurement employed in this work utilized a common three-level scheme where metastable Ar^{+*} is excited by laser radiation at 611.492 nm and decays with the emission of a 460.957 nm fluorescence photon (wavelengths given in vacuum) [12]. The LIF diagnostic used a pulsed dye laser (Sirah Cobra-Stretch) that was pumped by a frequency-doubled Nd:YAG laser ($\tau_{\mathrm{pulse}} = 3$ ns, $\lambda = 532$ nm, Spectra Physics Quanta-Ray). The experiment was run at 10 Hz. A schematic of the experimental arrangement and a photograph of the measured region are shown in Fig. 1.

The experimental bulk plasma was produced by a low frequency (600 kHz, 425 W) inductively coupled plasma (ICP) discharge. A higher frequency (2.2 MHz, 1.5 kW) capacitively coupled rf bias was applied simultaneously through a metal electrode inside a ceramic support structure holding the substrate; the vacuum chamber walls served as the path for currents to return to ground. This is depicted in Fig. 1. The rf voltage was measured at the base of the electrode assembly; the peak-to-peak amplitude was 1282 V. As there are measured stray impedances in the rf-bias feedthrough and electrode assembly, a deembed-
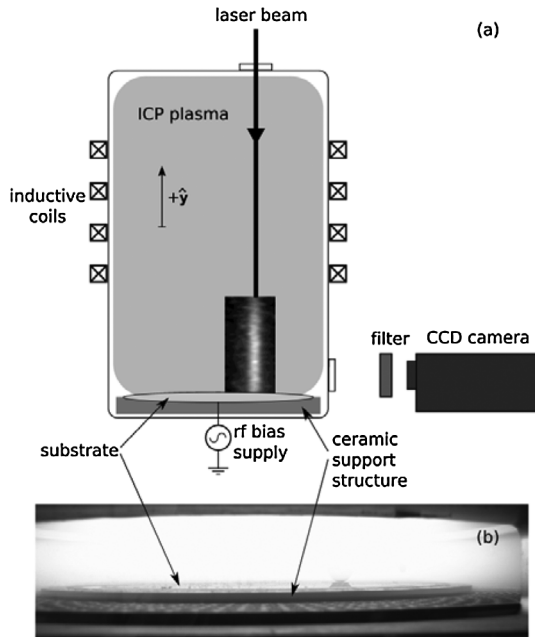
FIG. 1. (a) Experimental schematic: the laser beam is incident from the top of the machine such that the vertical IVDF can be acquired. The silicon substrate was supported by a ceramic structure with an embedded rf electrode referenced to the grounded chamber walls. A raw CCD image of the LIF light with the laser tuned to the resonance peak is shown in the inset (not to scale). (b) A photograph looking through the same window as the CCD camera shows the bright plasma above the substrate and the ceramic support structure below.

ding procedure [13] was performed to extract the actual voltage at the substrate surface; this produced a sheath voltage peak-to-peak amplitude of 1100 V.

Argon (80%) and oxygen (20%) were fed into the chamber, with a fill pressure of 0.5 mTorr. Oxygen was added to the argon discharge to prevent the deposition of opaque films on the vacuum windows. The LIF signal was reduced by less than 22% by the presence of oxygen. The laser beam (~1 cm diameter) passed through the top window, striking the substrate at normal incidence, 7.5 cm from its center. Fluorescence light from the illuminated plasma passed through a narrow ($\Delta\lambda = 1$ nm) bandpass interference filter to a fast ($\tau_{\text{exposure}} \geq 3$ ns) 14 bit CCD camera (Cooke Corporation DiCam-Pro). Each pixel in the 320×640 camera images corresponded to an area of 354 μm $\times$ 88.5 μm within the imaged plane. The laser pulse was phase locked to the rf-bias waveform with a timing jitter of about 2% of the period (10 ns) and LIF data was taken at 8 different phases. Timing was verified by monitoring the laser emission with a fast photodiode and the rf-bias current on an oscilloscope.

At 0.5 mTorr, the argon-ion mean free paths for charge exchange, ion-neutral collisions, and ionization processes are significantly greater than the measured sheath thickness ($s = 3.6$ mm). The ion continuity equation, $\Gamma(y) =$

$n(y)u(y) = $ const, dictates that ion density (and consequently the LIF signal) drops rapidly across the sheath due to the steep positive gradient in the ion velocity. Here, Γ is the ion flux, n is the ion density, and u is the ion flow velocity as functions of the distance y above the substrate. In order to obtain LIF measurements in the sheath with a useful signal-to-noise ratio, it was necessary to increase the laser intensity into the power saturation regime resulting in the equivalent of instrumentally broadened IVDF [12]. The ion velocity distribution is deconvolved from the measured distribution using a maximum entropy technique [14]. A further complication arises due to the partial reflection of the laser beam from the substrate surface [15] which produces an illusory "ghost" population of ions drifting away from the substrate. Consequently, in this work we show only the IVDF's of ions drifting downwards.

An rf-compensated Langmuir probe [16] was inserted into the bulk plasma to measure an electron temperature of $T_e = 1.6$ eV, a plasma potential of $V_p = 5.4$ V, and a bulk plasma density of $n_0 = 6.9 \times 10^{10}$ cm^{-3}. Typical bulk ion temperatures measured by LIF were 0.21 eV. A spatial average across the fluorescing region (horizontal extent $\delta x \cong 1$ cm), was taken at each position above the substrate and 1000 CCD images were taken at each laser wavelength.

Figure 2(a) shows the IVDFs at eight phases at a location deep within the sheath (only 1.06 mm above the substrate). The distribution functions are dramatically different at
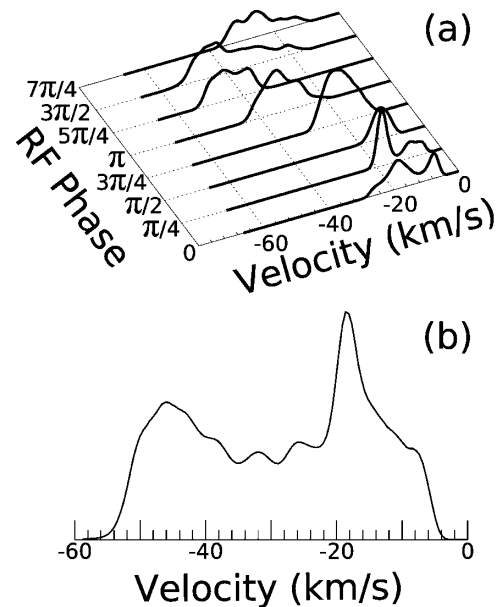
FIG. 2. (a) Time-resolved IVDFs measured by LIF at eight different phases of the 2.2 MHz rf bias, taken at a point 1.06 mm above the wafer substrate (sheath thickness is ~3.6 mm). (b) shows the time average of the IVDF data from (a). rf-bias voltage is most negative when the rf phase $\Phi = \pi$. Negative velocities indicate ions traveling down towards the substrate.

different phases, showing the extreme time dependence of the ion sheath dynamics in the intermediate frequency regime. The effect of the ion transit time is also evident in that the most energetic ions are observed not at the phase $\Phi = \pi$, when the sheath potential is most negative (maximum ion acceleration,) but are delayed by a phase shift of about $\pi/2$. The plasma processing system used in this experiment operates with the ratio of the ion transit time through the sheath to the rf period between 0.2 and 0.4; the actual value for the data discussed in this Letter is $\tau_{\text{ion}}/\tau_{\text{rf}} = 0.3$.

The 2.2 MHz rf-bias period is $\tau_{\text{rf}} = 455$ ns and the ion transit time of $\tau_{\text{ion}} = 130$ ns is estimated from reference [17]:

$$\tau_{\text{ion}} = 2\left(\frac{s^2 M_i}{2e\langle V_s\rangle}\right)^{1/2}\left[\left(1 + \frac{kT_e}{2e\langle V_s\rangle}\right)^{1/2} - \left(\frac{kT_e}{2e\langle V_s\rangle}\right)^{1/2}\right]$$

(1)

with M_i the ion mass, k the Boltzmann constant, e the unit charge, T_e the electron temperature, and $\langle V_s\rangle$ the time average of the voltage drop created by the rf bias. The quantity s is the sheath width, which was measured to be $s = 3.6$ mm $(+/-0.09$ mm, the pixel size): at this position the observed ion flow velocity (at all phases) equals the Bohm speed. Predictions of the sheath width [11] give

$$s \approx \frac{2}{3}\left(\frac{2e}{kT_e}\right)^{1/4}\left(\frac{\varepsilon_0}{0.61n_0 e}\right)^{1/2}\langle V_s\rangle^{3/4} = 3.1 \text{ mm.}$$

(2)

Time averaging the IVDF over all phases [Fig. 2(b)] yields bimodal distributions functions $f(v)$ similar to those reported by others [11,17].

Surface plots of the IVDF as a function of height above the substrate (y) are shown at two different phases in Fig. 3. The data in Fig. 3(a), obtained at the rf phase $\Phi = \pi/2$, show only relatively small drifts develop near the substrate surface, with the drift velocity reaching $v_y = -17$ km/s, exceeding the Bohm speed $c_s = 1.93$ km/s. Figure 3(b) shows data taken when $\Phi = 3\pi/2$, with the peaks of the distribution functions reaching $v_y = -47$ km/s. Both surfaces show a similar presheath for $y > 6$ mm, but are very different for $y < 4$ mm, the region of the rf sheath.

The LIF diagnostic was unable to measure IVDFs for $y < 1$ mm due to the low ion density in this region. At the substrate surface, $y = 0$, we expect that the IVDF shown in Fig. 3(b) extends to higher velocities, with maximum ion energy approaching the peak-to-peak sheath voltage drop of 1100 V [18].

Profiles of the ion flux $\Gamma = \int v f(v) \times dv (10^{10}$ cm^{-3} km/s) are shown in Fig. 4(a), ion flow velocities $u = \frac{\int v f(v) dv}{\int f(v) dv}$ (km/s) are shown in Fig. 4(b), and profiles of the heat flux $Q = M_i \int v^3 f(v) dv$(kW/m^2) in Fig. 4(c). Here v is the vertical component of the ion
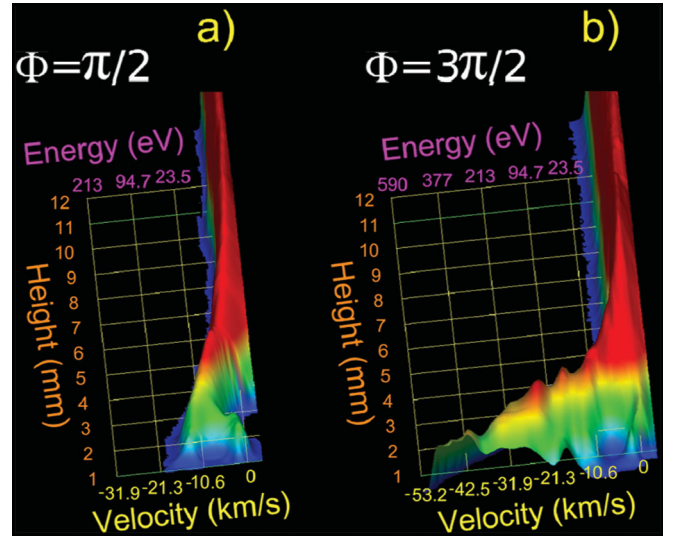
FIG. 3 (color). Experimental LIF data showing the IVDFs at two phases ($\Phi = \pi/2, 3\pi/2$) of the rf bias and as a function of height above the substrate. The 2.2 MHz bias power was 1.5 kW. The IVDFs are normalized at each height to better show the sheath structure. In (a) the presheath is visible as a gentle curve in the peak and high energy ions are not observed. In (b) ions of energy in excess of 500 eV are observed in the sheath nearest the substrate. The LIF diagnostic was unable to measure IVDFs for $y < 1$ mm.

velocity and $f(v)$ is the measured IVDF. The time-average ion flux throughout the sheath region is approximately constant at 4.34×10^{10} cm^{-3} km/s. The calculated Bohm flux is $\Gamma = n_s c_s$, with n_s the ion density at the sheath edge is 5.46×10^{10} cm^{-3} km/s. The flow velocities differ by as much as a factor of 4 as a function of rf phase, the heat flux is dominated by a contribution during one quarter of the rf cycle. Since the ion transit time is comparable to the rf period, there is a phase delay between the moment when the substrate is biased most negatively with respect to the bulk plasma and the observation of the fastest ions. The average heat flux has a linear profile in the sheath region: extrapolating in to the region $y < 1$ mm, the estimated time-average heat flux to the substrate is 16.8 kW/m^2.

We report for the first time detailed, spatially, and temporally resolved nonintrusive measurement of the ion velocity distribution $f(v)$ in the presheath and sheath region over a large (30 cm diameter) rf-biased substrate. The experiment was performed in the regime where the ion transit time through the sheath is on the order of the rf period ($\tau_{\text{ion}}/\tau_{\text{rf}} = 0.3$). Time averaging our measurements shows $\langle f(v)\rangle$ to be bimodal; this is in accord with predictions from models as well as previous time-averaged measurements. However, in this work large changes in the structure of the IVDF within the sheath are observed as a function of time during the rf cycle. The most energetic ions were observed shortly after the time of maximum ion acceleration (the time when the rf sheath potential is
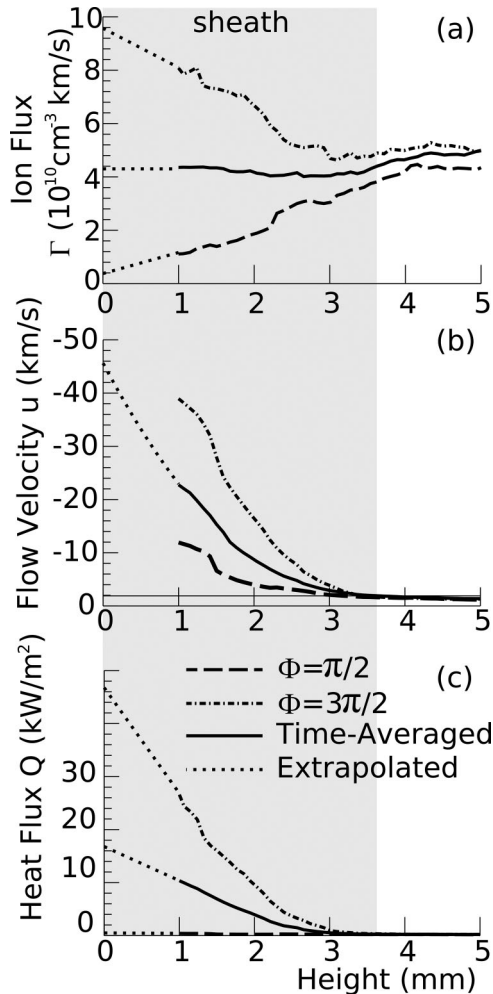
FIG. 4. Plots of (a) ion flux (b) ion flow velocity and (c) ion heat flux to the substrate versus height above the substrate calculated from the LIF data. The plasma density was measured with an rf-compensated Langmuir probe and used to calibrate the LIF diagnostic. The dashed curves show data from two different phases ($\pi/2$ and $3\pi/2$) of the rf-bias cycle; the thick solid curves are time averaged over an rf period. In (b), the thin horizontal line shows the Bohm velocity ($c_s = 1.93$ km/s). LIF data were not acquired for $y < 1$ mm; the dotted curves show extrapolations of the measured profiles into this region.

most negative), highlighting the importance of ion transit time effects. These results could be used in conjunction with sheath models to predict the IVDF at the substrate surface [17].

*Present Address: Applied Materials, Santa Clara, CA 95405, USA.
[1] S. Cowley et al. (Plasma 2010 Committee), NRC report, "Plasma Science: Advancing Knowledge in the National Interest," Plasma 2010 Report (National Academy Press, Washington, DC, 2007), Chap. II.
[2] R. McWilliams et al., Thin Solid Films **515**, 4860 (2007).
[3] D. B. Graves and M. J. Kushner, J. Vac. Sci. Technol. A **21**, S152 (2003).
[4] R. A. Stern and J. A. Johnson, Phys. Rev. Lett. **34**, 1548 (1975).
[5] F. Anderegg et al., Phys. Rev. Lett. **57**, 329 (1986).
[6] R. Stern, D. Correll, H. Boehmer, and N. Rynn, Phys. Rev. Lett. **37**, 833 (1976).
[7] N. Sadeghi et al., Appl. Phys. Lett. **70**, 835 (1997).
[8] B. Jacobs, W. Gekelman, P. Pribyl, M. Barnes, and M. Kilgore, Appl. Phys. Lett. **91**, 161505 (2007).
[9] K.-U. Riemann, Phys. Plasmas **4**, 4158 (1997).
[10] B. K. Woodcock et al., J. Appl. Phys. **81**, 5945 (1997).
[11] E. Kawamura, V. Vahedi, M. A. Lieberman, and C. K. Birdsall, Plasma Sources Sci. Technol. **8**, R45 (1999).
[12] M. Goeckner, J. Goree, and T. Sheridan, Rev. Sci. Instrum. **64**, 996 (1993).
[13] J. W. Butterbaugh, L. D. Baston, and H. H. Sawin, J. Vac. Sci. Technol. A **8**, 916 (1990).
[14] N. Agmon, Y. Alhassid, and R. D. Levine, J. Comput. Phys. **30**, 250 (1979).
[15] M. J. Goeckner, J. Goree, and T. E. Sheridan, Phys. Fluids B **4**, 1663 (1992).
[16] U. Flender et al., Plasma Sources Sci. Technol. **5**, 61 (1996).
[17] M. S. Barnes, J. C. Forster, and J. H. Keller, IEEE Trans. Plasma Sci. **19**, 240 (1991).
[18] M. A. Sobolewski, Phys. Rev. E **59**, 1059 (1999).